Inorganic Chemistry

Communication

pubs.acs.org/IC

# Monovalent and Mixed-Valent Potassium Salts of [1,2,5]Thiadiazolo[3,4-*f*][1,10]phenanthroline 1,1-Dioxide: A Radical Anion for Multidimensional Network Structures

Yoshiaki Shuku,[†] Rie Suizu,[†,‡] and Kunio Awaga*[,†,§]

[†]Department of Chemistry & Research Centre for Materials Science, Nagoya University, Furo-cho, Chikusa, 464-8602 Nagoya, Japan

[§]CREST, JST, Nagoya University, Furo-cho, Chikusa, 464-8602 Nagoya, Japan

Supporting Information

**ABSTRACT:** A novel phenanthlorine derivative, [1,2,5]-thiadiazolo[3,4-*f*][1,10]phenanthroline 1,1-dioxide ($tdapO_2$), was prepared to act as a radical-anion building block for coordination polymers. The crystal structures and magnetic properties of the monovalent and mixed-valent radical-anion salts $K{\cdot}tdapO_2$ and $K{\cdot}(tdapO_2)_2$ were elucidated and confirm the possibility of $tdapO_2$ to act as a bridging ligand and its capability to exhibit magnetic ordering at 15 K.

The magnetic and electrical properties of molecule-based materials have been extensively studied, and versatile phenomena have been discovered, such as molecular semiconductors/conductors/superconductors, nonlinear transport, magnetic ordering, paramagnetic−diamagnetic transitions, and low-dimensional magnetism.[1] In these research fields, radical species have been widely employed because the unpaired electrons are potential charge carriers and magnetization sources. In contrast to the chemical variety of cationic and neutral radicals, the development of radical-anion species has been very limited, probably because of their instability (oxidation) under ambient (oxygen) conditions. The most representative stable radical anions are $TCNQ^-$, $TCNE^-$, and $DCNQI^-$, which have been shown to form functional charge-transfer compounds with various cation radicals and metal ions.[2] It is notable that these anions have the duality of being both radical anions and ligands, and they often form a 3D network structure because of $\pi-\pi$ interactions and coordination bonds.[1a,3] It is, therefore, important to develop the methodology to stabilize radical-anion species and to expand their chemical variety.

The title molecule, [1,2,5]thiadiazolo[3,4-*f*][1,10]-][1,10]phenanthroline 1,1-dioxide (abbreviated as $tdapO_2$; see Scheme 1), was designed to possess a stable radical-anion species. The strong electron-withdrawing property of the thiadiazole dioxide moiety[4] enhances the acceptor ability of $tdapO_2$. In addition, the phenanthroline and thiadiazole dioxide moieties at the molecular ends are expected to operate as ligands and/or hydrogen-bond acceptors, which can realize multidimensional interactions. In the present report, we describe the syntheses of $tdapO_2$ and its monovalent and mixed-valent radical-anion salts of potassium, namely, $K{\cdot}tdapO_2$ and $K{\cdot}(tdapO_2)_2$.

**Scheme 1. Synthetic Route and Expected Multidimensional Interactions of $tdapO_2$**

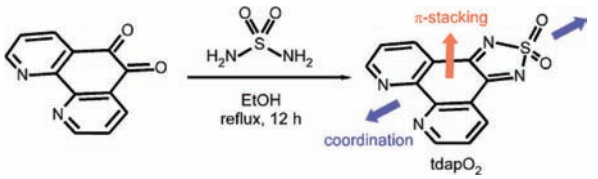


The molecule $tdapO_2$ was synthesized by a reaction between the diketone precursor (1,10-phenanthroline-5,6-dione)[5] and sulfamide $[(NH_2)_2SO_2]$ in ethanol (see Scheme 1). Yellow block crystals of $tdapO_2$ were obtained by sublimation. The molecular structure of $tdapO_2$ is shown Figure S1a in the Supporting Information (SI), and selected bond lengths are listed in Table 1. Figure S1b in the SI shows the crystal

**Table 1. Selected Bond Lengths of $tdapO_2$, $K{\cdot}tdapO_2$, and $K{\cdot}(tdapO_2)_2$**

| | | bond length/Å | | | |
|---|---|---|---|---|---|
| | | S−O[a] | S−N[a] | N−C[a] | C6−C7[b] |
| $tdapO_2$ | | 1.427 | 1.687 | 1.289 | 1.508 |
| $K{\cdot}(tdapO_2)$ | | 1.442 | 1.641 | 1.340 | 1.434 |
| $K{\cdot}(tdapO_2)_2$ | 1 | 1.429 | 1.692 | 1.294 | 1.503 |
| | 2 | 1.447 | 1.660 | 1.330 | 1.455 |

[a]Average of two nonequivalent bond lengths. [b]Carbon atoms belonging to the thiadiazole ring. See the SI (Figure S1).

structure of $tdapO_2$, which consists of a 2D layer formed by C−H···N hydrogen bonds. Figure S2 in the SI shows the highest occupied molecular orbital and lowest unoccupied molecular orbital (LUMO) of neutral $tdapO_2$, calculated by B3LYP methods, using 6-31G(d) basis sets.[6] These frontier orbitals are delocalized over the whole molecular skeleton. Figure 1 shows the cyclic voltammogram (CV) of $tdapO_2$, which indicates two reversible reduction peaks at −0.520 and −1.32 V vs $Fc^+/Fc$ (Fc: ferrocene); they suggest the stability of the mono- and dianion species of $tdapO_2$ and the acceptor ability of $tdapO_2$ to be comparable to those of the halogen-substituted *p*-benzoquinones.[7] It is notable that the related compound,

**Received:** September 8, 2011
**Published:** November 3, 2011

  

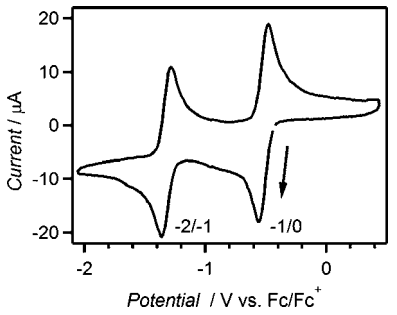


**Figure 1.** CV of 1 mM $tdapO_2$ in a $CH_3CN$ solution of 100 mM *n*-$Bu_4NClO_4$ at a scan rate of 100 mV $s^{-1}$.

[1,2,5]thiadiazolo[3,4-*f*][1,10]phenanthroline (tdap),[8] exhibits no reduction in the electrochemical window of $CH_3CN$. This means that the oxidation of sulfur in the thiadiazole ring notably reduces the reduction potential. Furthermore, the extent of delocalization of the LUMO is supported by the small potential separation ($\Delta E_{1/2}$) between the two reduction processes, similar to the case of nickel bis(dithiolenes),[9] suggesting that the monoanion radical is well distributed over the molecular skeleton, thus decreasing the Coulombic repulsion for subsequent reduction.

Crystals of a 1:1 salt, K·$tdapO_2$, were obtained by a slow diffusion method in an H-shaped glass cell. Figure 2 shows the

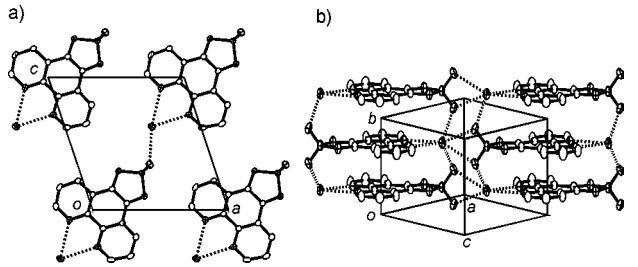


**Figure 2.** Crystal structure of K·$tdapO_2$: (a) projection of the unit cell along the *c* axis; (b) 2D network structure parallel to the (10−1) plane formed by $\pi$-stacking and coordination bonding.

crystal structure of this salt. The bond lengths of $[tdapO_2]^-$ are compared with those of the neutral molecule in Table 1. The most significant change is the shortening of the C6−C7 distance by 0.074 Å in $[tdapO_2]^-$. The bond distances in the thiadiazole dioxide moiety also exhibit characteristic changes, as shown in Table 1. These changes can be well explained by the bonding/antibonding features of the LUMO on these bonds. The length of the bonds with a bonding feature (N−C) shrinks, and those with an antibonding feature (S−N and C6−C7) expand after reduction.

The crystal structure of K·$tdapO_2$ consists of a coordination polymer chain along the $a + c$ direction (Figure 2a) and a 2D layer formed by $\pi$ stacking along the *b* axis with an interplanar distance of 3.30 Å (Figure 2b). As expected, the phenanthroline and thiadiazole dioxide moieties of $tdapO_2$ operate as coordination sites for different potassium ions, forming a coordination polymer structure. The potassium ion is surrounded by two nitrogen atoms and four oxygen atoms.

The temperature ($T$) dependence of the magnetic susceptibility of K·$tdapO_2$ was examined in the temperature range of 2−300 K. After compensating for the diamagnetic susceptibility, the temperature dependence of the paramagnetic susceptibility $\chi_p$ is shown in Figure 3a. With a decrease in the temperature from 300 K, $\chi_p$ shows a gradual increase. After a

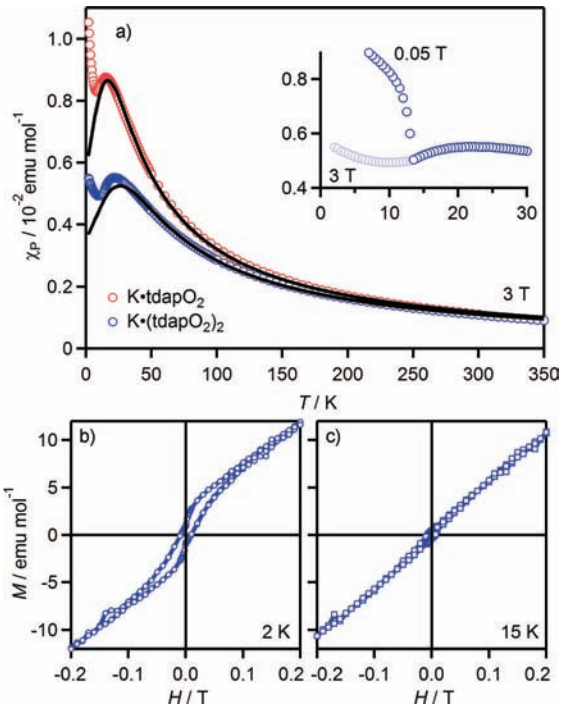


**Figure 3.** (a) Temperature dependence of the paramagnetic susceptibilities of K·$tdapO_2$ (red circles) and K·$(tdapO_2)_2$ (blue circles) under 3 and 0.05 T (inset). The solid curves show the theoretical fits to the data (see the text). (b and c) Magnetization curves of K·$(tdapO_2)_2$ at 2 and 15 K, respectively.

maximum is reached at 13.5 K, $\chi_p$ shows a decrease, followed by a quick increase again below 6.5 K. The latter behavior is probably caused by the Curie spins on the lattice defects. The $\chi_p$ values in the range of 16−300 K can be well fitted to the antiferromagnetic Bonner−Fisher model, assuming the spin Hamiltonian to be $H = -2J\sum S_i \cdot S_{i+1}$.[10] The solid curve on the open circles in Figure 3a is the theoretical best fit of this model with $g = 2.00 \pm 0.05$ and $J/k_B = -13 \pm 1$ K, where $g$ is the $g$ factor, $J$ is the antiferomagnetic coupling constant, and $k_B$ is the Boltzmann constant. The magnetization curves of this salt indicate no spontaneous magnetization even at 2 K (Figure S4 in the SI).

A mixed-valent 1:2 salt, K·$(tdapO_2)_2$, was prepared by galvanostatic electrocrystallization in a $CH_3CN$ solution containing $tdapO_2$ and K·$ClO_4$. Figure 4 shows the crystal

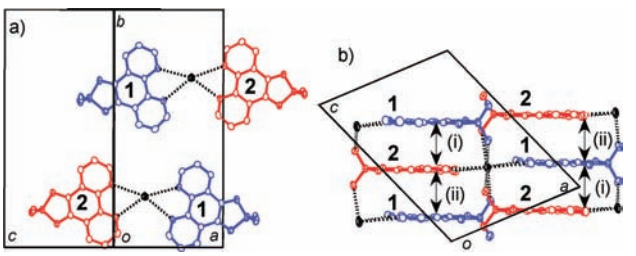


**Figure 4.** Projection of the crystal structures of K·$(tdapO_2)_2$ parallel (a) and perpendicular (b) to the $\pi$-stacking direction.


dx.doi.org/10.1021/ic201966t | *Inorg. Chem.* 2011, 50, 11859–11861

structure of K·(tdapO$_2$)$_2$, which consists of two crystallographically nonequivalent tdapO$_2$ molecules, **1** and **2**, with a significant difference in molecular structure. They form an alternating $\pi$-stacking arrangement along the $a + c$ axis, with very similar interplanar distances of 3.29 Å but different intermolecular arrangements (i and ii; see Figures 4b and S3b in the SI). As is shown in Figure 4a, a potassium ion is tweezered by the phenanthroline moieties of the coplanar molecules **1** and **2** in different $\pi$-stacking columns and is capped by the two thiazole dioxide moieties from both sides of the plane.

The bond parameters of **1** and **2** in K·(tdapO$_2$)$_2$ are listed in Table 1. A comparison with the neutral and anionic tdapO$_2$ molecules clearly indicates that **1** and **2** are in the neutral and radical-anion states, respectively. This salt is in a class I mixed-valence state[11] or, in the other words, in a charge-ordered state, a state that has attracted much attention in recent years.[12] Figure 4b indicates that the molecules **1** and **2** exhibit a checkerboard-type charge ordering.[13]

Figure 3a depicts the temperature dependence of $\chi_P$ for K·(tdapO$_2$)$_2$, where the molar unit contains two tdapO$_2$ molecules. The behavior in the temperature range from 33 to 350 K can be fitted to the Bonner−Fisher model with $g = 1.95 \pm 0.05$ and $J/k_B = -20 \pm 1$ K. This $|J|$ value is larger than that of K·tdapO$_2$, although the $\pi$-stacking column in K·(tdapO$_2$)$_2$ includes the nonmagnetic molecule **1**. Figure S3 in the SI shows the intermolecular overlap motifs in K·tdapO$_2$ and K·(tdapO$_2$)$_2$, indicating only slight differences between them. In general, the intermolecular magnetic exchange interaction results from cancellation between the ferromagnetic and antiferromagnetic contributions. Therefore, it is not very surprising that the antiferromagnetic interaction in K·(tdapO$_2$)$_2$ is stronger than that in K·tdapO$_2$ if the latter involves a stronger ferromagnetic contribution. Below 15 K, $\chi_P$ exhibits a sudden jump, followed by a Curie-like behavior. The field dependence of magnetization was measured at various temperatures. The results are shown in Figures 3b,c and S5 in the SI. The magnetization curves indicate the presence of small spontaneous magnetization below 15 K, which is probably caused by spin canting. This is one of the highest transition temperatures among those of the molecule-based magnetic materials that do not include transition metals.[14]

In summary, we have demonstrated the synthesis of the novel acceptor tdapO$_2$ and the crystal structures and magnetic properties of K·tdapO$_2$ and K·(tdapO$_2$)$_2$. The radical anion [tdapO$_2$]$^-$ was found to possess an ability to form $\pi$-stacking and coordination bonding. Because the radical/ligand anions can form close contacts with cationic metal ions, the present study strongly indicates the capability of tdapO$_2$ to exhibit a high potential as a building block in molecular magnetism and organic spintronics.

## ■ ASSOCIATED CONTENT

### Ⓢ Supporting Information

Crystallographic data in CIF format, crystal structures of neutral tdapO$_2$, computational calculation, magnetization curves of K·(tdapO$_2$)$_2$, experimental details, and details of crystallographic data. This material is available free of charge via the Internet at http://pubs.acs.org.

## ■ AUTHOR INFORMATION

### Corresponding Author

*E-mail: awaga@mbox.chem.nagoya-u.ac.jp.

### Present Address

‡Graduate School of Advanced Integration Science, Chiba University.

## ■ ACKNOWLEDGMENTS

The authors are grateful to the Ministry of Education, Culture, Sports, Science, and Technology (MEXT) of Japan for a Grant-in-Aid for Scientific Research. R.S. thanks the JSPS for a postdoctoral fellowship.

## ■ REFERENCES

(1) (a) Kobayashi, H.; Kobayashi, A.; Tajima, H. *Chem. Asian J.* **2011**, *6*, 1688−1704. (b) Miller, J. S. *Chem. Soc. Rev.* **2011**, *40*, 3266−3296. (c) Awaga, K.; Tanaka, T.; Shirai, T.; Fujimori, M.; Suzuki, Y.; Yoshikawa, H.; Fujita, W. *Bull. Chem. Soc. Jpn.* **2006**, *79*, 25−34. (d) Gütlich, P.; Koningsbruggen, P. J.; Renz, F. *Struct. Bonding (Berlin)* **2004**, *107*, 27−75. (e) Sato, O.; Tao, J.; Zhang, Y. *Angew. Chem., Int. Ed.* **2007**, *46*, 2152−2187. (f) Gatteschi, D. *Adv. Mater.* **1994**, *6*, 635−645.

(2) Conwell, E., Ed. *Semiconductors and semimetals*; Academic Press: New York, 1988; Vol. *27*.

(3) (a) Kaim, W.; Moscherosch, M. *Coord. Chem. Rev.* **1994**, *129*, 157−193. (b) Lopez, N.; Zhao, H.; Ota, A.; Prosvirin, A. V.; Reinheimer, E. W.; Dunbar, K. R. *Adv. Mater.* **2010**, *22*, 986−989. (c) Kato, R.; Kobayashi, H.; Kobayashi, A. *J. Am. Chem. Soc.* **1989**, *111*, 5224−5232.

(4) (a) Caram, J. A.; Mirífico, M. V.; Vasini, E. J. *Electrochim. Acta* **1994**, *39*, 939−945. (b) Caram, J. A.; Mirífico, M. V.; Aimone, S. L.; Vasini, E. J. *Can. J. Chem.* **1996**, *74*, 1564−1571. (c) Caram, J. A.; Mirífico, M. V.; Aimone, S. L.; Piro, O. E.; Castellano, E. E.; Vasini, E. J. *J. Phys. Org. Chem.* **2004**, *17*, 1091−1098. (d) Mirífico, M. V.; Caram, J. A.; Gennaro, A. M.; Cobos, C. J.; Vasini, E. J. *J. Phys. Org. Chem.* **2009**, *22*, 964−970.

(5) Yamada, M.; Tanaka, Y.; Yoshimoto, Y.; Kuroda, S.; Shimao, I. *Bull. Chem. Soc. Jpn.* **1992**, *65*, 1006−1011.

(6) (a) Petersson, G. A.; Bennett, A.; Tensfeldt, T. G.; Al-Laham, M. A.; Shirley, W. A. *J. Chem. Phys.* **1988**, *89*, 2193−2218. (b) Petersson, G. A.; Al-Laham, M. A. *J. Chem. Phys.* **1991**, *94*, 6081−6090.

(7) (a) Chambers, J. Q. In *The chemistry of the quinonoid compounds*; Patai, S., Ed.; John Wiley & Sons: New York, 1974. (b) Peover, M. E. *J. Chem. Soc.* **1962**, 4540−4549. (c) Davis, K. M. C.; Hammond, P. R.; Peover, M. E. *Trans. Faraday Soc.* **1962**, *61*, 1516−1522. (d) Ryba, O.; Pilař, J.; Petránek, J. *Collect. Czech. Chem. Commun.* **1968**, *33*, 26−34.

(8) Conte, G.; Bortoluzzi, A. J.; Gallardo, H. *Synthesis* **2006**, *23*, 3945−3947.

(9) Lim, B. S.; Fomitchev, D. V.; Holm, R. H. *Inorg. Chem.* **2001**, *40*, 4257−4262.

(10) (a) Kahn, O. *Molecular Magnetism*; Wiley-VCH: Weinheim, Germany, 1993. (b) Bonner, J. C.; Fisher, M. E. *Phys. Rev.* **1964**, *135*, A640−A658. (c) Estes, W. E.; Gavel, D. P.; Hatfield, W. E.; Hodgson, D. J. *Inorg. Chem.* **1978**, *17*, 1415−1421.

(11) Robin, M. B.; Day, P. *Adv. Inorg. Chem. Radiochem.* **1967**, *10*, 247−422.

(12) (a) Okamoto, K.; Tanaka, T.; Fujita, W.; Awaga, K.; Inabe, T. *Angew. Chem., Int. Ed.* **2006**, *45*, 4516−4518. (b) Okamoto, K.; Tanaka, T.; Fujita, W.; Awaga, K. *Phys. Rev. B* **2007**, *76*, 075328.

(13) Kimura, S.; Suzuki, H.; Maejima, T.; Mori, H.; Yamada, J.; Kakiuchi, T.; Sawa, H.; Moriyama, H. *J. Am. Chem. Soc.* **2006**, *128*, 1456−1457.

(14) Deumal, M.; Rawson, J. M.; Goeta, A. E.; Howard, J. A. K.; Copley, R. C. B.; Robb, M. A.; Novoa, J. J. *Chem.—Eur. J.* **2010**, *16*, 2741−2750.